ENVIRONMENTAL ENGINEERING SCIENCE
Volume 15, Number 1, 1998
Mary Ann Liebert, Inc.

The Effect of Cofiring High-Sulfur Coal with Municipal Waste on Formation of Polychlorinated Dibenzodioxin and Polychlorinated Dibenzofuran

BRIAN K. GULLETT,[1] K. RAGHUNATHAN,[2] and JAMES E. DUNN[3]

[1]*National Risk Management Research Laboratory (MD-65)*
U.S. Environmental Protection Agency
Research Triangle Park, North Carolina
[2]*Acurex Environmental Corporation*
P.O. Box 13109
Research Triangle Park, North Carolina
[3]*Department of Mathematical Sciences*
University of Arkansas
Fayetteville, Arkansas

ABSTRACT

The effect of cofiring minor amounts (5–10 wt %) of high-sulfur coal with municipal refuse–derived fuel (RDF) on emissions of polychlorinated dibenzo-*p*-dioxin (PCDD) and polychlorinated dibenzofuran (PCDF) was studied under a range of operating conditions. Through use of a 2^x factorial test matrix the program examined the effect of sulfur dioxide (SO_2) concentration on preventing PCDD/F formation while accounting for differences in hydrogen chloride concentration, sorbent slurry injection, and various furnace operating conditions such as quench rate, residence time, and RDF feed rate. An understanding of the effect of coal- and operating-related parameters on the postcombustion formation of PCDD/F is expected to assist in developing strategies aimed at preventing PCDD/F formation. The test facility was a 0.6-MW_t (2×10^6 Btu/h) pilot scale, grate-fired combustor, designed to mimic the solid fuel handling and combustion rates of field units.

Results were analyzed by examining comparative-run-averaged yields and through development of a model based on regression methods with stepwise parameter selection. The run-averaged yields and model show that higher SO_2 concentrations due to cofiring with coal result in significant suppression of PCDD/F formation, even when controlling for changes in other operating parameters.

Key words: Polychlorinated dibenzodioxin; polychlorinated dibenzofuran; PCDD; PCDF; waste combustion; refuse-derived fuel; coal; cofiring; sulfur dioxide; emissions

INTRODUCTION

FORMATION OF POLYCHLORINATED dibenzo-*p*-dioxins (PCDD) and polychlorinated dibenzofurans (PCDF) in waste and industrial combustors has led to international regulatory limitations on air emissions. However, measurements of PCDD/F yields from coal combustion suggest that these sources are relatively insignificant (Riggs et al., 1995) despite the apparent similarity in combustion conditions of temperature, surfaces, metal catalysts,

and trace products of incomplete combustion [the reader is referred to the recent review by Addink and Olie (1995) on mechanisms of PCDD/F formation].

Previous pilot scale research (Gullett and Raghunathan, 1997) has shown that formation of PCDD/Fs during coal combustion can occur but is limited by hydrogen chloride (HCl) concentration. In addition, the presence of sulfur dioxide (SO_2) has been shown to inhibit PCDD/F formation (Gullett et al., 1992; Raghunathan and Gullett, 1996), perhaps at least partially through the mechanism proposed by Griffin (1986) and supported by results of Raghunathan and Gullett (1996) in which an aromatic chlorinating agent (Bruce et al., 1991), chlorine (Cl_2), is supplied by the catalyst-aided reaction:

$$2HCl + 1/2O_2 \leftrightarrow Cl_2 + H_2O$$

but depleted by the presence of SO_2:

$$Cl_2 + SO_2 + H_2O \leftrightarrow 2HCl + SO_3$$

Another candidate mechanism for the inhibition of PCDD/F formation by sulfur species has been discussed (Gullett et al., 1992) in which the catalyst activity [represented below by copper (Cu) species] is poisoned or altered by reaction with SO_2:

$$CuO + SO_2 + 1/2O_2 \rightarrow CuSO_4$$

The product copper sulfate ($CuSO_4$) is a less active catalyst than cupric oxide (CuO) for the production of Cl_2 through the Deacon process, as well as for the biaryl synthesis step of PCDD/F formation.

Other potential reasons for lower observed PCDD/F yields in coal combustors are improved combustion efficiency resulting in insignificant organic precursors as products of incomplete combustion (PICs), potential coal-borne mineral matter interactions with catalysts or Cl concentrations, and formation of polychlorodibenzothiophenes and polychloroanthrenes [the analogs to PCDFs and PCDDs, respectively, in which the O atom(s) are replaced by S atom(s)].

Lindbauer et al. (1992) reported that cofiring coal in a municipal solid waste (MSW) incinerator led to appreciably lower PCDD/F levels. Manninen et al. (1996) undertook a multiparameter study in a facility that cofired up to 26% (thermal) RDF with coal. Their work took the approach of supplementing coal with RDF (our work focuses on supplementing RDF with coal) and conducting a multivariate analysis of the combustion parameters and yield results. They found that the ratio of SO_2/HCl (varied through changes in HCl) was inversely proportional to PCDD/F formation, although tests with direct application of elemental sulfur to the grate were ineffective. Recently, Ogawa et al. (1996) compared the effect of adding gaseous SO_2 versus generating SO_2 through coal addition and found the latter to be more effective. Thus, there may be other benefits with coal cofiring than simply being a source of SO_2.

This work scales up our previous efforts in the laboratory (Gullett et al., 1992) and waste combustor simulator (Raghunathan and Gullett, 1996) to a pilot scale, RDF waste combustion trial. This trial attempts to answer the intriguing question, what is the effect of cofiring minimal amounts of coal in waste-fired systems that are known to produce PCDD/F? This effort intends to validate the suppression of PCDD/F formation with coal/RDF cofiring while accounting for mechanistic effects of other operating parameters. Tests were conducted over a range of process variables (e.g., calcium hydroxide [$Ca(OH)_2$] injection, HCl concentration, flue gas temperature, quench, and residence time) so that the results could have implications for a wide variety of waste combustors.

EXPERIMENTAL

Tests were run in the EPA's Multi-Fuel Combustor (MFC) facility (Fig. 1), rated at 0.6 MW (2×10^6 Btu/h) thermal output, and capable of burning a wide variety of solid fuels including MSW, RDF, biomass, and coal. The modular design of the facility provides flexibility for studies on various pollutant emissions and control and for solid fuels with unknown firing and handling characteristics. The MFC consists of a waste feeding system, a coal feeder, a lower combustion chamber containing a stoker, a radiant section, a convective flue gas passage, a baghouse, and a wet scrubber system. In addition, there is a separate fuel preparation system for shredding, screening, and mixing the fuel. A large loading hopper conveys the processed fuel to the fuel silo.

As indicated in Figure 1, there are two ports for flue

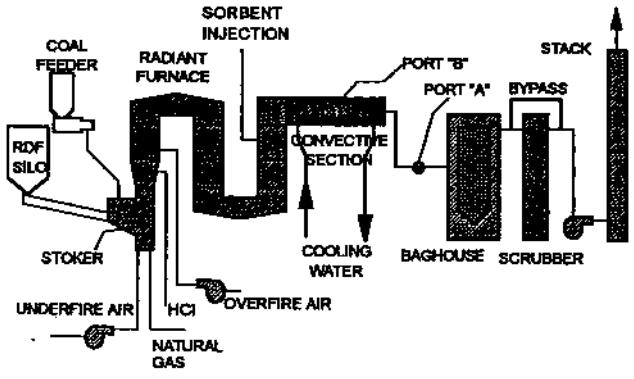

FIG. 1. Schematic of the Multi-Fuel Combustor (MFC).

gas sampling and temperature measurements along the convective section and the duct. The convective section is equipped with cooling coils for high-pressure water circulation. The cooling oil originally present in location B was removed for this project, to accommodate PCDD/F sampling. A typical temperature drop across the convective section is from 600°C to 150°C, which includes the PCDD/F formation "window" (200–500°C). The residence time and quench rate across this window is known to be an important parameter, and it can be varied in our tests by changing the temperature set point of the cooling water. From the convective section, flue gas was sampled through continuous emission monitors (CEMs) for recording the oxygen (O_2), carbon dioxide (CO_2), carbon monoxide (CO), HCl, and SO_2 concentrations.

The primary fuel for the MFC consisted of a commercial, densified RDF derived from processed municipal waste. The coal was an Illinois No. 6 coal (donated by Monterey Coal Company, Carlinville, IL) ground and classified to an average diameter of about 1 mm. The coal was fed using a screw feeder and entered the burner at the same location as the RDF. Analyses of the RDF and coal are shown in Table 1. For runs with sorbent injection, a commercial hydrated lime [$Ca(OH)_2$] was injected as a slurry at a nominal Ca/Cl stoichiometric ratio of 1.5:1.

The experimental parameters varied in the tests were:

RDF feed rate—LOW or HIGH
Coal feed—ON or OFF
Quench—LOW or HIGH
Sorbent injection—ON or OFF
HCl gas addition—ON or OFF

The experiments were structured to provide information on all main effects and two-factor interactions among the above parameters for statistical modeling. The design test matrix conditions are shown in Table 2. A total of 30 tests, including blanks, were run with various parameter settings. The resultant test condition simple statistics are shown in Table 3.

During each test, the fuel feed rate was adjusted whenever necessary to maintain a constant flue gas temperature throughout the radiant section of the furnace. For low-RDF feed runs, natural gas was cofired to compensate for the decrease in heat release and to maintain similar temperature ranges between runs. Quench was varied by changing the temperature set point of the cooling water used in the convective section of the furnace. For runs with gaseous HCl addition, there was about a 150

TABLE 1. ANALYSES OF THE REFUSE-DERIVED FUEL (RDF) AND ILLINOIS NO. 6 COAL

Factor	*RDF*	*Coal*
Proximate analysis (%)		
Moisture	7.33	14.96
Ash	8.46	8.32
Volatile matter	71.20	33.51
Fixed Carbon	12.94	43.21
Ultimate analysis (%)		
Moisture	7.33	14.96
Carbon	41.74	60.25
Hydrogen	5.56	4.22
Nitrogen	0.58	1.09
Sulfur	0.09	3.36
Ash	8.46	8.32
Oxygen (by difference)	36.20	7.80
Other Element analysis (%)		
Chlorine	0.22	0.09
Calcium	1.35	n.m.
Copper	0.002	n.m.
kJ/kg	16,408	25,257
(Btu/lb)	(7,059)	(10,866)

n.m. = Not measured.
Values may not add to 100% due to rounding.

TABLE 2. TEST MATRIX DESIGN CONDITIONS

Run no.	*RDF rate*	*SO_2 (coal rate)*	*Sorbent rate*	*Added HCl*	*Quench rate*
7	H	N	N	N	H
9	H	N	N	N	L
11	HL	Y	N	N	H
12	L	N	N	N	L
13	H	N	N	N	L
14	H	N	N	Y	L
15	H	N	N	Y	H
18	L	N	N	N	L
19	L	N	N	Y	L
20	L	N	N	N	H
21	L	N	N	Y	H
23	L	N	N	Y	H
24	H	Y	N	N	L
25	H	Y	N	Y	L
26	L	Y	N	N	L
27	H	Y	N	N	H
28	H	N	Y	N	H
29	L	N	Y	N	H
30	L	N	Y	N	L
31	H	N	Y	N	L
32	H	N	Y	Y	L
34	H	N	Y	Y	H
35	L	N	Y	Y	L
36	L	N	Y	Y	H
37	H	Y	Y	N	L

Missing run numbers are incomplete tests.
H, high; L, low; HL, medium; Y, yes; N, no.

TABLE 3. TEST CONDITION STATISTICS

Parameter	*Minimum*	*Maximum*	*Average*	*Median*
RDF feed rate, **RDF** (kg/min)	0.257	1.931	0.974	1.115
SO_2 concentration, **SO2** (g/min)	0.000	6.709	1.607	0.011
Sorbent rate, **CA** (g/min)	0	10.8	NA	NA
HCl concentration, **HCL** (g/min)	0.254	5.000	2.367	1.958
Quench rate, **QU** (C°/s)	304	531	420	426
Sampling temp., **TS** (°C)	146	380	256	246
Port A PCDD/F yield (ng/min)	0	8887	1033	326
Port B PCDD/F yield (ng/min)	26	10477	1536	446

NA = Not applicable. Sorbent was either ON or OFF.

ppm increase in flue gas HCl concentration. The sorbent slurry feed rate was about 0.6 kg solids/h and the injection temperature was approximately 700°C.

The flue gas was sampled from two locations (A and B in Fig. 1, prior to the air pollution control devices) for PCDD/F according to EPA Method 23 (1991) with an approximate sampling duration of 2 h. Before and after running Method 23 trains, a velocity traverse of the duct was carried out to measure the flue gas flow rate. The samples were analyzed in EPA's inhouse Organics Support Laboratory (OSL), via procedures described elsewhere (Gullett et al., 1993).

DATA ANALYSIS

For each test, temperature and flue gas composition data were stored in a data acquisition system. Run averages of these data were calculated for the duration of PCDD/F sampling, so that these values correspond to the measured yields. With the total flue gas flow rate known from the velocity traverse data, the average flue gas temperature profile data were used to determine the flue gas residence times at the sampling ports. In the temperature profiles, the residence time variable, t_R, is set to zero at 650°C. The choice of 650°C stems from the fact that most PCDD/F formation is known to take place below this temperature. The quench rate values were determined by fitting an exponential equation to the temperature/time values and solving for the slope at a temperature, 350°C, implicated for high rates of PCDD/F formation.

Conventionally, for comparative analysis, emission data are normalized to a specific O_2 concentration (e.g., 7%) to decouple possible differences in flue gas dilution between tests. In this work, however, for tests with LOW RDF feed rate, the co-fired natural gas (and its stoichiometric combustion air), effectively dilutes the flue gas, but without the equivalent increase in O_2. Thus, normalizing the PCDD/F data with 7% O_2 would underestimate the PCDD/F yields attributed to the LOW RDF feed rate. Therefore, data were modeled in temporal rate form (units of ng PCDD/F/min) and presented as such or, when normalized to the RDF feed rate, presented in terms of units of ng PCDD/F/kg RDF. These fuel feed rates could not be measured during the experiments and had to be determined by solution of mass balance equations for O_2, CO_2, and total flue gas flow rates with the data on the composition, combustion stoichiometry, and flue gas flow rate (note that these rates reflect cumulative yields and, as such, should not be considered as instantaneous rates of reaction).

RESULTS

The range, average, and median tetra- to octa-PCDD and -PCDF yield results for the tests performed in this work are given in Table 3. Due to fluctuations in the RDF feed rate and the possible inherent variations in the RDF composition, the flue gas composition exhibited fluctuations throughout a run. Gas composition values for each run were determined by the average value during the sampling period. For most of the runs, the CO levels from RDF burning were low (about 12 ppm), indicating good combustion quality. Results from three of four natural-gas-only runs (as system blanks) showed minimal levels of PCDD and PCDF. One blank run early in the test program resulted in unexpectedly high values; these values were attributed to residual effects from the previous run (an RDF HIGH run) and preceded procedural modifications which established rigorous between-run, duct cleanout procedures.

STATISTICAL ANALYSIS

The yields of total PCDD + PCDF, tetra- to octachlorinated congeners, for each port A and B, expressed

TABLE 4. DEFINITIONS OF MODEL PREDICTORS

Potential predictors	*Definition*
INT	Intercept
HCL	HCl concentration, g/min
SO2	SO2 concentration, g/min
RDF	RDF feed rate, kg/min
TS	Sample port temperature, °C
CA	Sorbent rate, 0 if sorbent not used, 10.8 g/min if sorbent used
QU	Quench rate at 350°C, C°/s
SO2vHCL	**SO2/HCl**, unitless
SO2vHCl2	**(SO2/HCl)^2**, unitless
RDF2	**RDF * RDF**
HCLvRDF	**HCL/RDF**, g HCl/kg RDF
SO2vRDF	**SO2/RDF**, g SO2/kg RDF
QUHCLvRDF	**QU * HCL/RDF**
Interactive predictors:	
SO2RDF	**SO2*RDF**
SO2QU	**SO2*QU**
SO2CA	**SO2*CA**
SO2HCL	**SO2*HCL**
RDFQU	**RDF*QU**
RDFCA	**RDF*CA**
RDFHCL	**RDF*HCL**
QUCA	**QU*CA**
QUHCL	**QU*HCL**
CAHCL	**CA*HCL**

as ng/min were collectively modeled through selection among 23 potential predictors defined in Table 4. Hereafter, the model predictors are shown in boldface as per Table 4 notation. To better model the data, an optimal transformation for total yield was determined from choices involving logarithmic and power transformations using exponents 0.25, 0.30, 0.35, and 0.40. An optimal transformation to the 0.35 power was determined. The subsequent model-predicted values are termed **TOTAL$^{0.35}$** and their transform to **TOTAL** is comparable to the sampled yields of total PCDD + PCDF, tetra- to octa-chlorinated congeners. The 23 predictors were made available for stepwise selection using SAS® procedure REG (the parameter residence time was omitted from the available list of predictors because its value was missing for runs 18, 19, and 26). The regression coefficients were estimated by generalized least squares, to account for pairwise, nonzero correlations between port A and port B responses. The best seven-predictor model (see Table 5) for a transformed **TOTAL** response was determined, based on a maximized R^2 criterion and minimization of p values for the partial effects of each predictor. The normal quantile-quantile (Q-Q) plot of the residuals (not shown) was nearly ideal, being linear and symmetric with respect to the origin. The compactness of the scatter about the line representing perfect prediction is reflected by $R^2 = 0.770$.

Data from several runs were flagged a priori as abnormal. Run 8 was dismissed because the CEM system malfunctioned and reliable gas concentrations were not obtained. Run 14 was suspect due to high CO values (indicative of poor fuel combustion) and eventually was dropped. Similarly, run 11 was flagged (high CO values) and runs 35 and 36 were flagged (atypically low filter–bound particulate matter recovery). All of the suspect runs (except run 8) were analyzed for potential inclusion or exclusion using Q-Q plots with their values flagged (plots not shown). Yields for runs 8 and 14 were identified as clear outliers and were excluded from further consideration. However, based on the relative position of data for runs 11, 35, and 36, these three runs were deemed consistent with the model reported here.

MODEL DISCUSSION

The model R^2 value (0.770, Table 5) suggests that the seven-predictor model accounts for 77% of the observed variation in PCDD/F values. The estimated correlation between the upstream yields (port B) and the downstream yields (port A) is about 0.676.

The relative influence of each parameter within the model can be assessed by calculation of the model R^2 in the absence of each parameter and by the squared semipartial correlation of each parameter. In Table 6, the effect of singly dropping each parameter from the model is observed by the reduction in model R^2 from the full-parameter model (0.770, Table 5). The amount of the observed variation in **TOTAL** that can be accounted for by variation of each specific parameter over its observed range can be estimated by the parameter-specific squared semipartial correlation.

The comparatively minor influences of **TS** and **HCL** on the model is observed by the minimal reduction in model R^2 when each respective parameter is removed from the model. Conversely, loss of **RDF** or **QU** has a major influence; the values of R^2 drop tremendously. The parameters in Table 6 are in rank order of importance to the model.

The squared semipartial correlations (Table 6) likewise show the relative importance of each parameter. Both **RDF** and **QU**, followed then by **CA** and **SO2**, can account for a large range of the observed **TOTAL** simply through variation across their experimentally observed range.

TABLE 5. MODEL PARAMETERS AND STATISTICS

Predictor	*DF*	*Coefficient estimate*	*Standard error*	*T for H0: C.E. = 0*	*Prob > [T]*
HCLvRDF	1	3.693468	1.23608483	2.998	0.0047
SO2RDF	1	−0.961880	0.19234349	−5.001	0.0001
RDFCA	1	−1.124311	0.23561975	−4.772	0.0001
QUHCLvRDF	1	−0.00804016	0.00293373	−2.741	0.0090
TS	1	0.00895978	0.00261982	3.420	0.0014
RDFQU	1	0.0230327	0.00217059	10.611	0.0001
QUCA	1	0.00188426	0.00060460	3.117	0.0033
Model R^2	0.7698		Port A, port B correlation		0.67596

Model predictions of **TOTAL** (through $\mathbf{TOTAL}^{0.35}$) are accomplished by summing the products of the regression coefficients (Table 5) with the predictor values, the latter being calculated by substitution of the appropriate parameters (as defined in Table 4).

Exercising the fitted model allows the effect of individual parameters to be examined through their variation over the range of observed test values while holding constant other parameters that affect **TOTAL**. Typically parameters held constant are set at their median observed values, unless noted (the **TS** value used is the median value for port B only). This approach is followed below to examine the effects of individual parameters. The partial effects of each parameter can be examined by partial differentiation of **TOTAL** with respect to the particular parameter. In this manner, the rate of change of **TOTAL** with respect to that parameter can be easily assessed.

SO2 The effect of increases in **SO2** is to decrease yields of PCDD/F throughout the full range of SO_2 values tested in this work. Figure 2 shows that increases in **SO2** cause reductions in **TOTAL** and that the magnitude of this effect is affected by **RDF**; when **RDF** is high, **TOTAL** is high and the deleterious effect of **SO2** is more striking than at low **RDF**. No other examined parameters were interactive with this effect.

QU and HCL The direct effect of **QU** is observed in Figure 3, and as a secondary parameter in Figures 4 and 5. At low values of **HCL** (such as the median tested value), Figure 4 shows that increases in **QU** result in increases in **TOTAL**. This is contrary to reported experimental testing (references) and to field observations based on mitigating measures. At higher values of **HCL** (above about 3.5 g/min), increases in **QU** result in the commonly observed reductions in **TOTAL**.

Figure 4 clearly shows an interesting interaction between **QU** and **HCL**. Increases in **HCL** result in increases in **TOTAL** if **QU** is not too high; the changes in $\mathbf{TOTAL}^{0.35}$ with respect to **RDF**-normalized **HCL** (**HCLvRDF**) are such that **TOTAL** will increase as long as **QU** does not exceed the ratio of the coefficients for **HCLvRDF** and **QUHCLvRDF**, 3.69/0.008, or about 461 C°/s. This value is about 40 C°/s higher than the median values found in these tests.

TS The model-predicted effect of sampling temperature on **TOTAL** is straightfoward. Increases in the sampling temperature, **TS** (see Fig. 6), show minor but significant increases in **TOTAL**. This is predicted by the temperature effect on $\mathbf{TOTAL}^{0.35} = 0.0896 * \mathbf{TS}$. Thus, the rate of change of $\mathbf{TOTAL}^{0.35}$ with respect to changes

TABLE 6. SEMIPARTIAL CORRELATIONS FOR MODEL PARAMETERS

Removed predictor terms	*Resultant model R^2*	*Parameter dropped from model*	*Squared semipartial correlation*
HCLvRDF, SO2RDF, RDFCA, QUHCLvRDF, RDFQU	0.006	**RDF**	0.764
QUHCLvRDF, RDFQU, QUCA	0.008	**QU**	0.762
RDFCA, QUCA	0.471	**CA**	0.299
SO2RDF	0.536	**SO2**	0.234
HCLvRDF, QUHCLvRDF	0.638	**HCL**	0.132
TS	0.754	**TS**	0.016

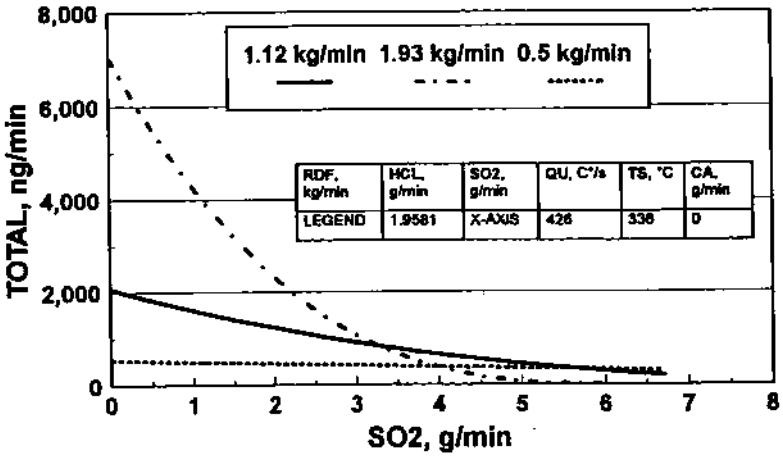

FIG. 2. Modeled effect of SO2 on TOTAL.

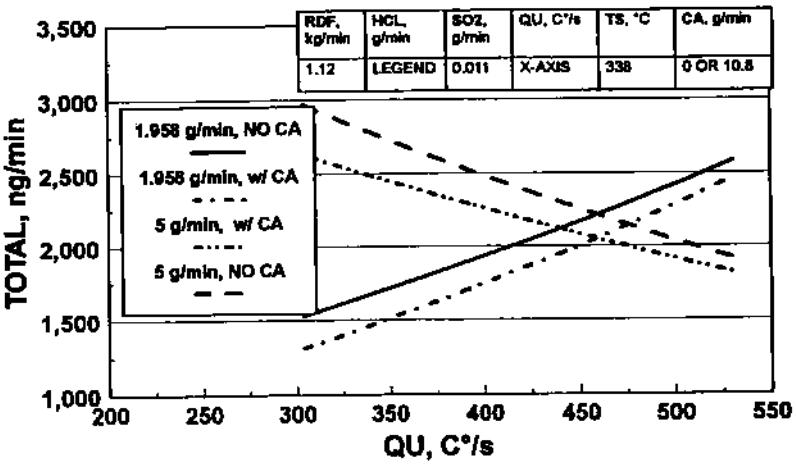

FIG. 3. Modeled effect of QU on TOTAL, HCL and CA variant.

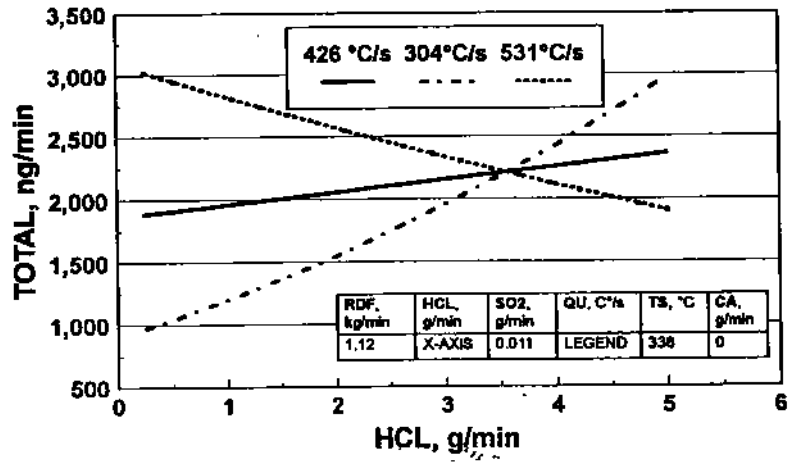

FIG. 4. Modeled effect of HCL on TOTAL, QU variant.

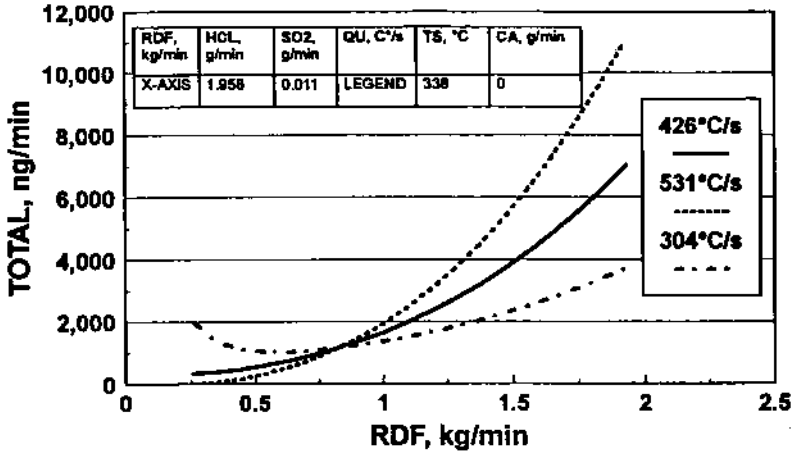

FIG. 5. Modeled effect of RDF on TOTAL, QU variant.

in TS is constant, 0.00896. This fairly minor effect of temperature is indicative of processes whose rates are strongly diffusion-dependent.

RDF The effect of increasing **RDF** is to increase **TOTAL**$^{0.35}$ throughout the full range of tested values. Increasing **RDF** from the median value of 1.12 kg/min to the maximum tested value results in increasing **TOTAL** from near-zero to values exceeding 2000 ng/min (Fig. 5). The **TOTAL**$^{0.35}$ dependency on changes in **RDF** is interactive with most other tested parameters, namely **HCL, SO2, CA,** and **QU**. The effect of **QU, RDF** interaction variation on **TOTAL** effect is also shown in Figure 5. Higher values of **QU** result in higher values of **TOTAL**$^{0.35}$. This phenomenon was examined earlier under **QU** and **HCL** discussions.

The **RDF** effect does not change much even when the Cl within the **RDF** (and hence, **HCL/RDF**) remains constant. Figure 7 shows that increasing **RDF** with commensurate increase in **HCL** in order to maintain a constant ratio results in a response much the same as that of Figure 5 in which **HCL** remained constant.

CA The effect of sorbent is examined as a secondary parameter in Figure 3 [since the experimental matrix was only set up with two conditions for **CA** (no sorbent or 10.8 g/min), it is inappropriate to examine a range of **CA** values]. The **TOTAL**$^{0.35}$ dependency on **CA** is also affected by **RDF** and **QU**. This dependency results in decreases in **TOTAL**$^{0.35}$ with increases in **CA**; this affect is accentuated by higher **RDF**. However, higher values of **QU** minimize the reductive effect of sorbent injection. The conflicting effects of **RDF** and **QU** cancel when **RDF** = 0.00188/1.124 * **QU** = 0.00167 * **QU**.

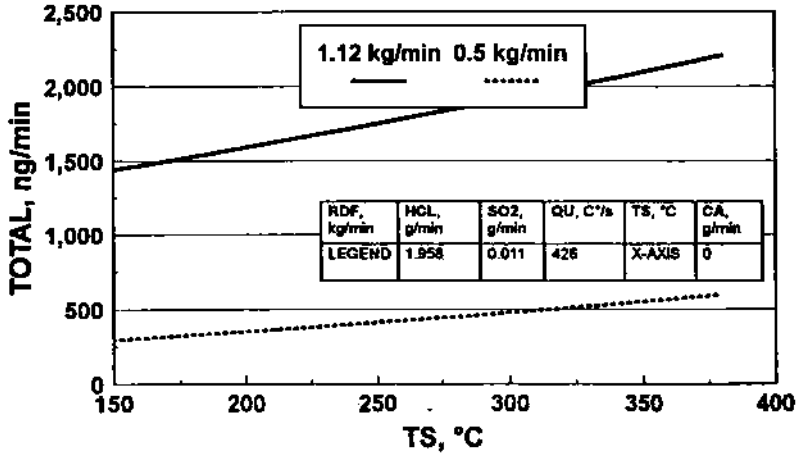

FIG. 6. Modeled effect of TS on TOTAL.

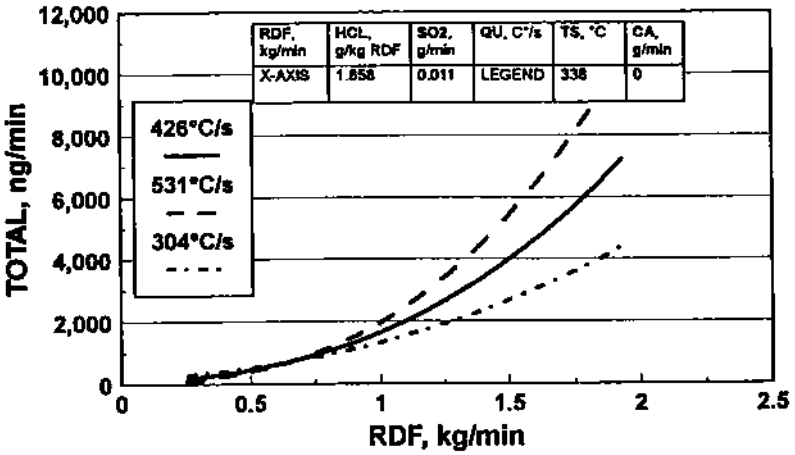

FIG. 7. Modeled effect of RDF on TOTAL, QU variant, HCL/RDF constant.

DISCUSSION

The values of sampled PCDD/F yield in these experiments are comparable to those expected for field measurements of raw flue gas. The RDF-only runs exhibited average tetra- to octa-PCDD/F yields of 615 ng/dscm.

An average analysis of all the experimental data has been performed, combining the data from sampling ports A and B. The data are divided into three groups—RDF only, RDF with coal cofiring, and RDF with sorbent injection—although within a group other parameters, such as HCl concentration, may vary. For each group, the average normalized PCDD/F yield is computed for each congener class. Results are plotted for tetra- to octa-PCDD and PCDF congener classes in Figure 8. As is typical of RDF combustion, the PCDFs were more abundant than the PCDDs, with an averge ratio of 1.4:1. Examination of the average congener distribution for RDF only shows that the dominant congener classes (tetra- to octa-PCDD/F) were the HxCDD and the tetra- to penta-CDF (TrCDF when including the mono- to tri-PCDF). Both coal cofiring and sorbent injection effect decreases in PCDD/F formation; their congener class patterns are similar to that of the base RDF case and, therefore, the reduction is not congener class–specific. The total tetra-octa PCDD and PCDF yields for the three groups are plotted in Figure 9. The results clearly indicate that coal/RDF cofiring as well as calcium-based sorbent injection reduces PCDD/F formation.

The observations from the average-run, sorbent effects (Fig. 9) in reducing PCDD/F formation are not as clearly supported by the modeling results. The modeling effort suggests that changes in other parameters during sorbent injection are partially responsible for the observed reductions. In this manner, the statistical, multiparameter analysis has separated out and accounted for simultane-

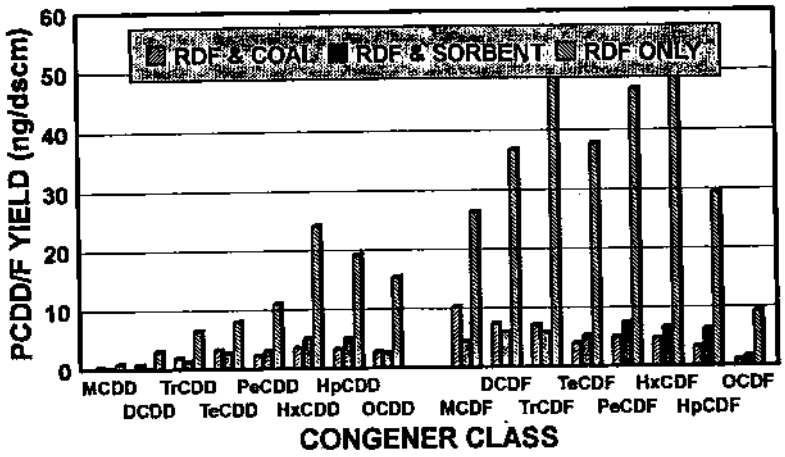

FIG. 8. Effects of coal cofiring and sorbent injection on PCDD/F congener class yields.

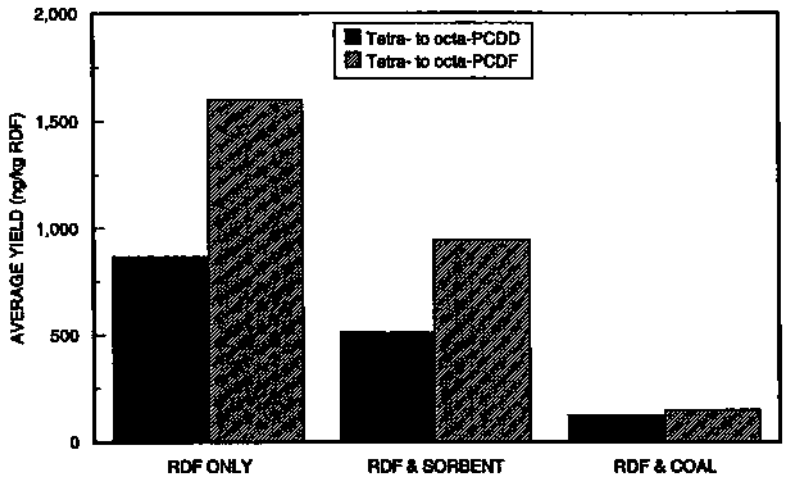

FIG. 9. Effects of coal cofiring and sorbent injection on average YIELD.

ous changes in operating conditions and parameters that affect formation of PCDD/F.

The modeled effect of **SO2/HCL** is observed in Figure 10. At moderate to low values of **QU**, substantial reduction in PCDD/F yield is observed throughout the illustrated range of **SO2/HCL**. The average flue gas **SO2/HCL** (mass) ratio for our coal-cofired tests was about 1.5. From Figure 2, an **SO2** value of 4 g/min seems to produce minimal **TOTAL**; this corresponds to an S/Cl molar ratio of about 1.1. For our test conditions this suggests that operation of the Multi-Fuel Combustor with about 5 wt % coal will result in significant yield suppression.

At high values of **QU**, the **SO2/HCL** trend reverses and higher values produce greater values of **TOTAL**. This is an unanticipated effect associated with **QU** (see discussion relating to Fig. 3). The oddity surrounding the behavior of **QU** may simply be due to an artifact of the method of its calculation or may be due to a complex interaction of competing formation and destruction reactions. At any rate, this phenomenon bears further investigation. The effect of SO_2/HCl can also be examined from a model derived from 47 measurements at 11 grate-fired RDF combustors (Huang and Buekens, 1995). These researchers developed a multiparameter quadratic model with $R^2 = 0.891$ between PCDD/F formation and gas concentration parameters plus fly ash loading. Calculations from their model show that yields of PCDD/F would decrease with increases in SO_2 when $SO_2/HCl < 0.7$. Their less complex models, however, do not predict reductions in yield as SO_2 increases.

The **RDF** response is not surprising except for the fact

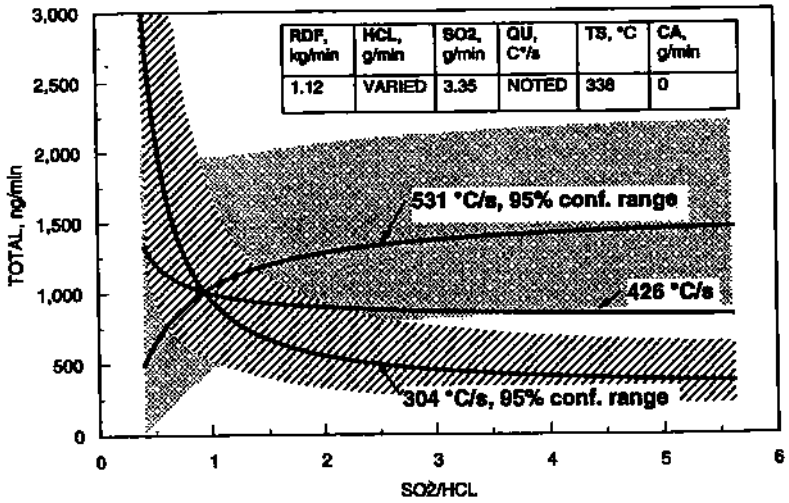

FIG. 10. Modeled effect of **SO2/HCL** on **TOTAL**, **QU** variant. Confidence limits (95%) shown for high and low **QU** values.

that these increases occur without simultaneous increases in the temporal concentration of **HCL** (g HCl/min). This suggests that there is plenty of HCl present (which also supports the weak influence of **HCL** in the model) and that yield increases in the presence of higher **RDF** feed rates are due to an increased supply of catalysts or organic precursors from incomplete combustion.

The changes in **TOTAL** response with respect to changes in the parameter values suggest that a complex interaction of formation and destruction reactions may occur in which the rate-controlling step changes throughout a run and possibly from run to run. This underscores the difficulty of making global statements regarding effects on PCDD/F yields of varying certain parameters.

Some questions remain regarding the effect of coal cofiring on PCDD/F formation suppression. It is not clear as to whether the effect of coal cofiring is simply to improve combustion conditions and reduce PCDD/F precursor concentrations; this work attempted to equalize combustion conditions (e.g., radiant section temperature) and account for operating parameter variation but did not rigorously measure trace combustion byproducts. If one can assume that CO concentration can be used as a rough monitor of combustion efficiency, it does not appear from our CO data that the mechanism of PCDD/F suppression during coal co-firing is due to improved fuel burnout. In fact, the average CO concentration was 7 ppm during RDF-only runs but increased to 43 ppm during cofired runs. It is additionally possible that mineral matter constituents the coal (which would be added to the combustor at a rate proportional to the SO_2 concentration) may have been the true mechanistic actors through sequestering of Cl or reduction of catalytic activity. Other questions relate to the mechanism of action and remain to be explored. In particular, the mechanism of PCDD/F suppression may be due to formation of chlorinated thiophenes and anthrenes instead of the chlorinated dioxins and furans.

CONCLUSIONS

This work has used similar-run, PCDD/F yield averaging along with statistical modeling to demonstate that cofiring RDF with about 5 wt % high-sulfur coal can result in significant suppression of PCDD/F formation at other than high quench rates. The model sufficiently accounts for variation in other parameters such as sampling temperature, RDF-specific flue gas, quench rate, and HCl concentration to demonstrate that these reductions in PCDD/F formation may likely be due to increased flue gas SO_2 concentrations from coal cofiring.

ACKNOWLEDGMENTS

This work was cosponsored by the Illinois Clean Coal Institute (ICCI) (Project Manager: Ken Ho) and the National Renewable Energy Laboratory (NREL) (Project Monitor: Phil Shepherd). Logistical support from Richard Valentine (U.S. EPA/APPCD) is greatly appreciate. Suh Lee, Joey Valenti, Russell Logan, Scott Moore, John Foley, Dennis Tabor, and Ann Preston (Acurex Environmental Corporation), and Jeff Ryan (U.S. EPA/APPCD) provided extensive technical, sampling, and analytical assistance.

DISCLAIMER STATEMENT

Any opinions, findings, conclusions, or recommendations expressed herein do not necessarily reflect the view of the ICCI, who sponsored this work in part. A detailed disclaimer from ICCI is available upon request.

REFERENCES

ADDINK, R., and OLIE, K. (1995) Mechanisms of formation and destruction of polychlorinated dibenzo-*p*-dioxins and dibenzofurans in heterogeneous systems, *Environ. Sci. Technol.*, **29**(6), 1425.

BRUCE, K.R., BEACH, L.O., and GULLETT, B.K. (1991) The role of gas-phase Cl_2 in the formation of PCDD/PCDF during waste combustion, *Waste Management*, **11**, 97–102.

GRIFFIN, R.D. (1986) A new theory of dioxin formation in municipal solid waste combustion, *Chemosphere*, **15**, 1987.

GULLETT, B.K., BRUCE, K.R., and BEACH, L.O. (1992) Effect of sulfur dioxide on the formation mechanism of polychlorinated dibenzodioxin and dibenzofuran in municipal waste combustors, *Environ. Sci. Technol.*, **26**(10), 1938.

GULLETT, B.K., LEMIEUX, P.M., and DUNN, J.E. (1993) Role of combustion and sorbent parameters in prevention of polychlorinated dibenzo-*p*-dioxin and polychlorinated dibenzofuran formation during waste combustion, *Environ. Sci. Technol.*, **28**(1), 107.

GULLETT, B.K., and RAGHUNATHAN, K. (1997) Observations on the effect of process parameters on dioxin/furan yield in municipal waste and coal systems, *Chemosphere*, **34**, 1027–1032.

HUANG, H., and BUEKENS, A. (1995) Analyzing dioxin measurement data in municipal waste incineration using multiple regression analysis, *Organohalogen Comp.*, **23**, 455–460.

LINDBAUER, R.L., WURST, F., and PREY, T. (1992) Combustion dioxin suppression in municipal solid waste incineration with sulfur additives, *Chemosphere*, **25**, 1409.

MANNINEN, H., PERKIIÖ, A., VARTIAINEN, T., and RUUSKANEN, J. (1996) Effect of fuel and fly ash composition on the formation of PCDD/PCDF in the co-combustion of refuse-derived and packaging-derived fuels, *Environ. Sci. Pollut. Res.* 3(3), 129–134.

Method 23 (1991) *Title 40 Code of Federal Regulations*, Part 60, Appendix A, U.S. Government Printing Office, Washington, DC.

OGAWA, H., ORITA, N., HORAGUCHI, M., SUZUKI, T., OKADA, M., and YASUDA, S. (1996) Dioxin reduction by sulfur component addition, *Chemosphere*, **32**, 151.

RAGHUNATHAN, K., and GULLETT, B.K. (1996) Role of sulfur in reducing PCDD and PCDF formation, *Environ. Sci. Technol.*, **30**(6), 1827.

RIGGS, K.B., BROWN, T.D., and SCHROCK, M.E. (1995) PCDD/PCDF emissions from coal-fired power plants, *Organohalogen Comp.*, **24**, 51–54.

Please address correspondence to:
Brian K. Gullett, Ph.D.
Air Pollution Prevention and Control Division (MD-65)
National Risk Management Research Laboratory
U.S. Environmental Protection Agency
Research Triangle Park, NC 27711

E-mail: bgullett@engineer.aeerl.epa.gov